

Characterization of various commercial forms of ammonium paratungstate powder

A. K. BASU, F. R. SALE

Department of Metallurgy, University of Manchester, Manchester, UK

The structures and morphologies of various commercial forms of ammonium paratungstate have been studied and related to the processes used for the production of this material. High temperature crystallization processes are shown to produce the monoclinic pentahydrate $5(\text{NH}_4)_2\text{O} \cdot 12\text{WO}_3 \cdot 5\text{H}_2\text{O}$ which yields a cuboid or equiaxed monoclinic powder morphology. Crystallization at room temperature produces the orthorhombic undecahydrate $5(\text{NH}_4)_2\text{O} \cdot 12\text{WO}_3 \cdot 11\text{H}_2\text{O}$ which has a lath-like particle morphology. Freeze-dried ammonium paratungstate is shown to be amorphous in nature, to have a chemical composition approaching that of the undecahydrate, and to have a porous, multiparticulate agglomerate particle morphology. The apparent densities of the samples of ammonium paratungstate are explained in terms of the particle morphologies.

1. Introduction

The production of solid ammonium paratungstate (APT) is an essential intermediate purification step in the overall extraction of tungsten from its naturally occurring ores scheelite, CaWO_4 , and Wolframite, $\text{Fe, Mn}(\text{WO}_4)$ [1]. The particle size and morphology of APT is particularly important in the production of tungsten powder, for either powder metallurgical uses or for the production of carbide material for the cutting tool industry, because these parameters may have marked effects on the properties of the metal powder. Tungsten metal is produced from APT by a thermal decomposition reaction, which gives tungsten trioxide for subsequent reduction by hydrogen. Consequently, particular attention is paid to the morphology of APT because of the possibility of producing the tungsten metal in the form of "pseudo-morphs" of the original APT particles.

Tungsten and its alloys are currently receiving extensive attention for the production of materials with improved strength and ductility over extended temperature ranges. Moreover, ultrafine tungsten powders, because of their unusual sizes and surface characteristics, may have unique applications as catalysts, fillers, fuels, nucleation agents in alloy production and other diverse applications, as well as in the more conventional fields of the hard-metals industry. Various new processes have been devised for the production of fine tungsten powders, and these

range from the hydrogen reduction of tungsten hexachloride vapour, which is produced directly by chlorination of the tungsten-bearing ore or residue [2], to the production and subsequent reduction of freeze-dried APT solutions [3-6].

A study is presently being made of the kinetics and products of the decomposition and hydrogen reduction of various commercial forms of APT with a view to optimizing the production of fine metal powders and evaluating the freeze-drying process. However, a vital and necessary initial part of this study has been a full characterization of the various commercial forms of this compound with particular reference being paid to particle size and morphology, crystal structure and apparent density.

2. Experimental procedure and results

2.1. Materials preparation

The five commercial samples of APT were manufactured following the conventional method of adding excess ammonia to a solution of tungstic acid. Sample 1 was produced by this technique and the resultant solution was slowly neutralized with hydrochloric acid at room temperature to yield solid APT. Sample 2 was manufactured by a similar technique except that the hydrochloric acid was used to neutralize a hot solution of tungstic acid in excess ammonia. Sample 3 was obtained by evaporation of a solution of ammonia and tungstic acid at its boiling point, whilst sample 4 was produced by

neutralization of the solution of tungstic acid and ammonia with hydrochloric acid at 75°C; however, the neutralized solution was subsequently held at this temperature for up to 6 h to allow the complete crystallization process to take place. Sample 5 was obtained by freeze-drying a solution of excess ammonia with tungstic acid by a conventional freeze-drying route.

The purity of all the samples of APT was found to be that required for the commercial use of this material. Table I shows a typical analysis of the impurity elements in these samples.

TABLE I Typical impurity analysis of the ammonium paratungstate samples

| Element | Concentration (%) |
|--|-------------------|
| Si | <0.005 |
| Ca | <0.005 |
| Al | <0.02 |
| Mg, Fe, Mo, Cr, Ni, Mn, Pb, B, Bi, Sn, Ti, V, Co | <0.01 |
| Ta | <0.10 |
| Nb | <0.05 |
| Na | 0.005 |

2.2. Weight loss on heating

A "Stanton" automatic thermobalance and a glass spring thermobalance were used to investigate the weight loss of the five samples on heating in a nitrogen atmosphere. The results given below are the averages of three determinations for each sample:

| | |
|---------------------|---|
| APT sample 1: 14.4% | } occurring over the temperature range 150 to 300°C |
| 2: 13.1% | |
| 3: 12.9% | |
| 4: 11.6% | |
| 5: 14.6% | |

2.3. Apparent density

The tap density of the five samples was determined in the standard manner [7].

| |
|---------------------------------------|
| APT sample 1: 1.46 g ml ⁻¹ |
| 2: 2.06 g ml ⁻¹ |
| 3: 2.03 g ml ⁻¹ |
| 4: 2.48 g ml ⁻¹ |
| 5: 1.03 g ml ⁻¹ |

2.4. X-ray diffraction analysis

X-ray diffraction examinations have been carried out on the five APT samples using CuK α

TABLE II *d*-spacings and intensities of the major lines obtained for sample 1

| <i>d</i> -spacing (Å) | <i>I</i> / <i>I</i> ₁ | <i>d</i> -spacing (Å) | <i>I</i> / <i>I</i> ₁ |
|-----------------------|----------------------------------|-----------------------|----------------------------------|
| 12.2 | 90 | 3.16 | 90 |
| 9.7 | 75 | 3.11 | 40 |
| 9.01 | 50 | 2.99 | 100 |
| 3.58 | 50 | 2.83 | 50 |
| 3.40 | 20 | 2.51 | 40 |
| 3.28 | 50 | 2.38 | 20 |

TABLE III *d*-spacings and intensities of the major lines obtained for samples 2, 3 and 4

| <i>d</i> -spacing (Å) | <i>I</i> / <i>I</i> ₁ | <i>d</i> -spacing (Å) | <i>I</i> / <i>I</i> ₁ |
|-----------------------|----------------------------------|-----------------------|----------------------------------|
| 10.30 | 100 | 3.02 | 30 |
| 8.56 | 30 | 2.97 | 50 |
| 5.15 | 60 | 2.89 | 50 |
| 4.89 | 25 | 2.64 | 20 |
| 3.23 | 60 | 2.51 | 40 |

radiation with a "Siemens Kristalloflex" diffractometer scanning over the range 6 to 80°. Samples 2, 3 and 4 gave the same major *d*-spacings which are listed in Table II. Sample 1 gave a different diffraction pattern and produced the major *d*-spacings given in Table III. In contrast to the other four samples, however, the freeze-dried APT (sample 5) failed to give an X-ray pattern of any form.

2.5. Particle size and morphology

All samples of APT were sieved in the "as-received" condition using an "Endecotts" sieve stack before examination with a "Cambridge" scanning electron microscope. Sample 1 was sticky and tended to form agglomerates on the first few sieves during shaking which gave above average percentages of oversize material on these sieves compared to samples 2 and 3. Sample 5 can be seen to contain a large amount of material of average diameter greater than 76 μ m, whilst sample 4, which had been graded by the manufacturer before distribution, was found to consist completely of particles of between 10 and 53 μ m average diameter. The results of the sieve analyses of samples 1, 2, 3 and 5 are presented in Table IV.

Specimens of the five samples were prepared for examination in the scanning electron microscope. In some cases the powders were sprinkled on to adhesive copper tape, which was attached to the standard aluminium specimen stub, prior to vacuum coating with aluminium.

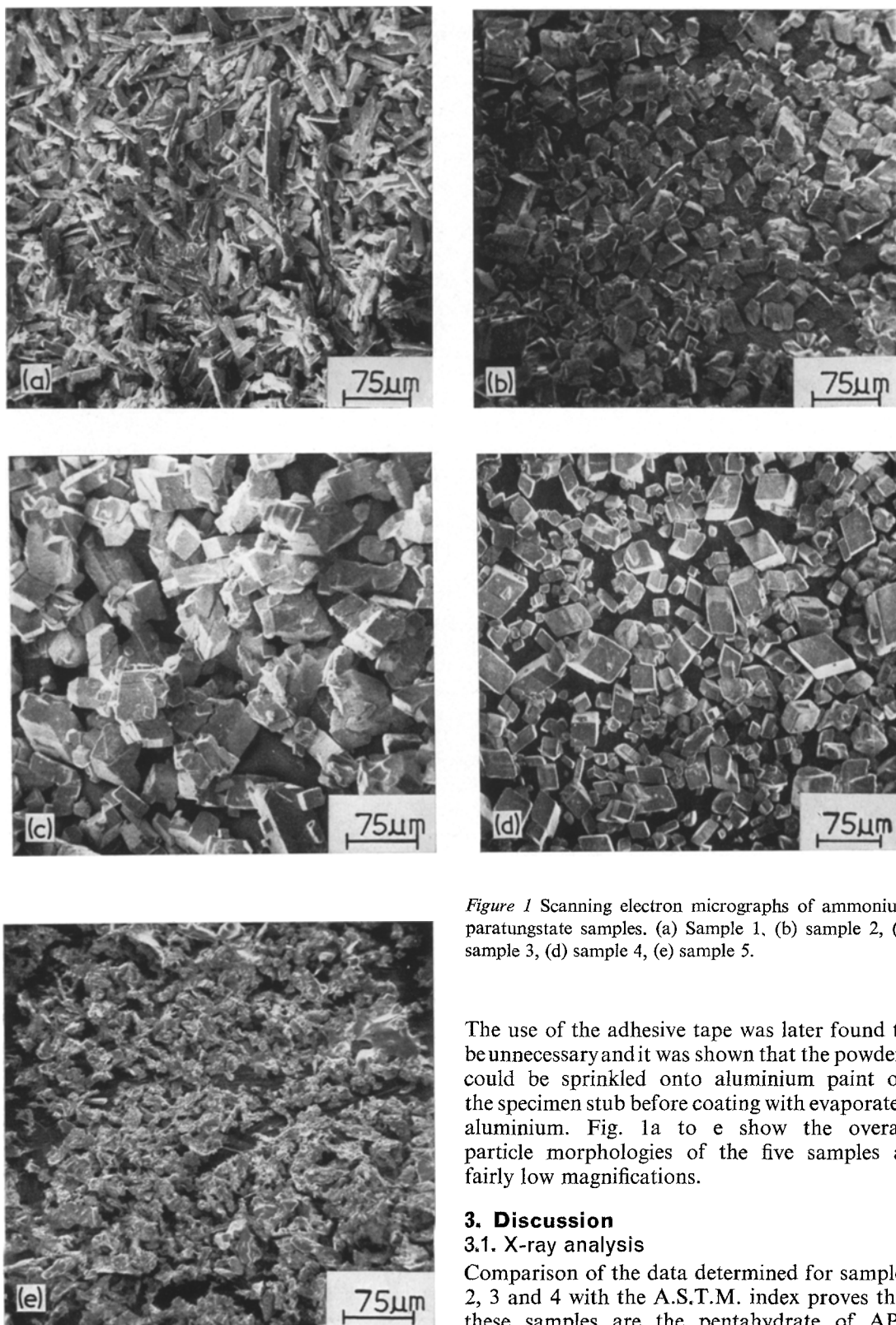


Figure 1 Scanning electron micrographs of ammonium paratungstate samples. (a) Sample 1, (b) sample 2, (c) sample 3, (d) sample 4, (e) sample 5.

The use of the adhesive tape was later found to be unnecessary and it was shown that the powders could be sprinkled onto aluminium paint on the specimen stub before coating with evaporated aluminium. Fig. 1a to e show the overall particle morphologies of the five samples at fairly low magnifications.

3. Discussion

3.1. X-ray analysis

Comparison of the data determined for samples 2, 3 and 4 with the A.S.T.M. index proves that these samples are the pentahydrate of APT

TABLE IV Sieve analysis for ammonium paratungstate samples

| Mesh size (μm) | Wt % retained Sample | | | |
|-----------------------------|-------------------------|------|------|------|
| | 1 | 2 | 3 | 5 |
| 699 | 19.2 | 1.3 | 8.3 | 10.5 |
| 251 | 2.8 | 0.4 | 3.2 | 26.6 |
| 152 | 15.8 | 0.5 | 14.2 | 21.4 |
| 76 | 13.6 | 16.1 | 40.4 | 22.5 |
| 53 | 11.1 | 18.2 | 20.8 | 10.5 |
| < 53 | 37.5 | 63.3 | 12.7 | 8.5 |

($5(\text{NH}_4)_2\text{O} \cdot 12\text{WO}_3 \cdot 5\text{H}_2\text{O}$), which has a monoclinic structure. The data for sample 1, however, shows this material to be the undecahydrate ($5(\text{NH}_4)_2\text{O} \cdot 12\text{WO}_3 \cdot 11\text{H}_2\text{O}$ – mis-named in the A.S.T.M. index as the hexadecahydrate), which has an orthorhombic structure, and so it is apparent that the low temperature neutralization and precipitation process produces a crystal form of APT which contains a greater degree of combined water than the higher temperature products. This has implications in the subsequent processing of this material in that lower process yields will result from its use, and higher particle pressures of water vapour may occur during the decomposition and reduction processes, with a consequential effect on the reduction path from tungsten trioxide to tungsten metal [8, 9], if a single stage decomposition/reduction process is used.

The X-ray diffraction data for the freeze-dried material (sample 5) indicate that it is amorphous in nature, and is, therefore, likely to behave in a different manner to the other samples during subsequent processing to yield the metal. Such amorphous products of freeze-drying have been reported previously [3], and were attributed to a particle size of the order of 20 to 40 Å. The freeze-dried material investigated in this study, however, contains particles of sizes up to 152 μm average diameter and the X-ray analyses were carried out on sieved material in the size range 75 to 53 μm .

The X-ray analyses of the five samples, which have indicated the higher combined water content of sample 1, explains the higher weight loss on heating obtained for this material by the thermogravimetric analysis. In fact the predicted weight loss due to decomposition of the undecahydrate to give tungsten trioxide (WO_3) is 14.1%. Similarly the predicted weight loss for the decomposition of the pentahydrate to give

tungsten trioxide is 11.2%. Slightly larger weight losses are to be expected in reality because the actual decomposition products have been shown by X-ray diffraction to consist of a mixture of WO_3 and $\text{WO}_{2.9}$. The predicted weight losses for samples 1 and 4, therefore, agree well with the observed data. The values for samples 2 and 3 indicate that a mixture of the various hydrated forms may be present in these specimens. On this basis, however, it appears that the freeze-dried material contains the same amount of combined water as the undecahydrate sample, which indicates that this process has not given an anhydrous product.

3.2. Particle size and morphology

The sieve analyses data presented in Table IV for samples 1, 2, 3 and 5, show that in the "as-received" condition sample 2 contains the largest percentage of particles of less than 53 μm average diameter. Only sample 4, which was a previously graded sample, contained a greater proportion of material less than 53 μm average diameter. Sample 1 yielded only approximately half the amount of material less than 53 μm average diameter obtained for sample 2. This could be due to both the sticky nature and the particle morphology of this sample. The freeze-dried material was very friable and was easily reduced in particle size on extended handling. Table V shows the sieve analysis of freeze-dried

TABLE V Sieve analysis of sample 5 after mild agitation (spatula stirring)

| Mesh size (μm) | Wt % Retained |
|-----------------------------|------------------|
| 699 | 0 |
| 251 | 0.2 |
| 152 | 8.9 |
| 76 | 39.0 |
| 53 | 16.9 |
| < 53 | 35.0 |

APT after a small amount of agitation. It can be seen that the proportion of particles less than 53 μm average diameter has increased dramatically. Similar agitation of the other samples caused a negligible change in particle size distribution. The extremely friable nature of the freeze-dried material indicates that a decrease in particle size may be expected during subsequent processing due to both mechanical handling and the decomposition and reduction reactions [10].

The particle morphology of the freeze-dried

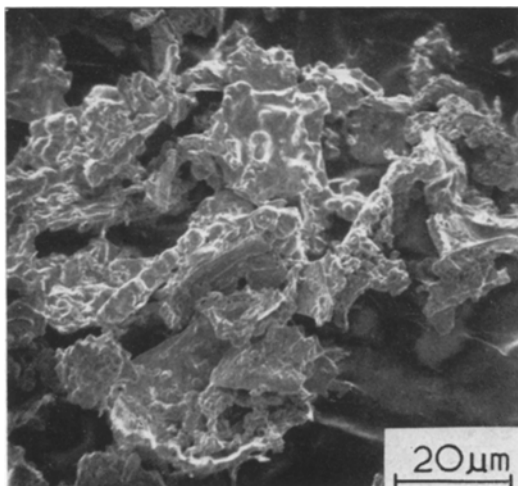


Figure 2 Freeze-dried ammonium paratungstate showing a multiparticulate morphology (sample 5).



Figure 3 Lath-like morphology of ammonium paratungstate (sample 1).

APT, as viewed in the scanning electron microscope (Fig. 1e), can be seen to be multiparticulate in nature and to possess no well-defined crystal shape. Fig. 2 shows this material at a higher magnification and the multiparticulate nature is demonstrated more clearly. This morphology explains the friability of the sample observed in the sieve analysis, and also demonstrates why there is such a difference in the apparent densities of the freeze-dried and conventionally-crystallized samples. An advantage of this morphological form may arise in the hydrogen reduction stage of subsequent processing in which the conventional commercial practice is to reduce the tungsten oxide in trays which are drawn through a furnace containing a hydrogen atmosphere. The porous nature of the freeze-dried material should dramatically increase both the access of the reducing gas to the solid oxide and the removal of the gaseous product of reduction from the reaction site.

Fig. 1a shows sample 1 to consist of lath-like crystals of varying dimensions. The particle sizes range from 16 to 70 μm in length and from 2 to 14 μm in width. At high magnification, (Fig. 3), it is evident that these crystals have been formed by the addition of thin layers, in typical stepwise crystal growth, along the top surface and leading edge of the crystal. This growth results in the formation of thick lath-like crystals of approximately rectangular cross-section. A comparison of the morphology of sample 1 with the cuboid, or equiaxed monoclinic, morphology of the closely-sized sample 4 indicates the reason

for the difference in tap densities of these two samples. The particle size in sample 4 can be seen to range from 10 to 50 μm with some evidence of even smaller particles adhering to the surfaces of some of the larger particles as shown in Fig. 4.

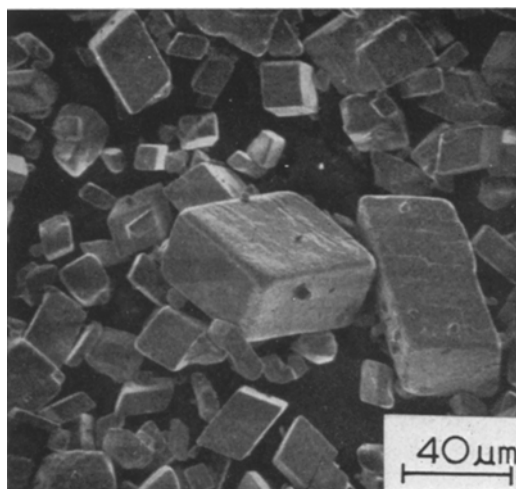


Figure 4 Cuboid, or equiaxed monoclinic, form of ammonium paratungstate crystals.

Samples 2 and 3, which have been shown to have the same crystal structure as sample 4 by the X-ray diffraction analysis, can be seen to be basically cuboid, or equiaxed monoclinic, in morphology in Fig. 1b and c respectively. The particle morphology in these samples, however,

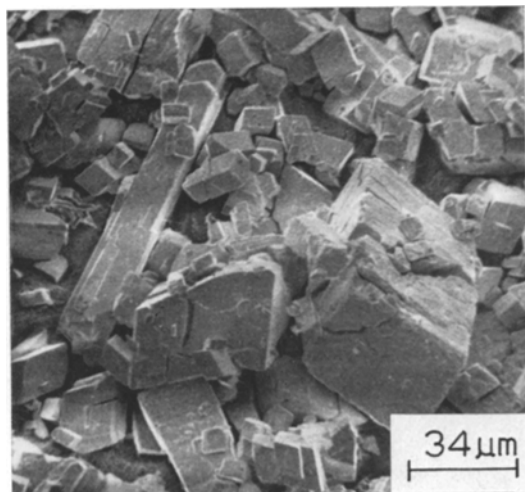


Figure 5 Sample 2 showing mainly equiaxed monoclinic crystals with a small amount of lath-like material.

can be seen to be not as perfect as that of sample 4. There is evidence that sample 2 contains a small amount of the lath-like form of APT, see Fig. 5; however, the proportion of this material was too small to be detected in the X-ray analysis. The small amount of the $5(\text{NH}_4)_2\text{O} \cdot 12\text{WO}_3 \cdot 11\text{H}_2\text{O}$ crystals were presumably produced as the original hot neutralized solution cooled whilst the crystallization process was still occurring.

As mentioned earlier the crystal shape of samples 2 and 3 is not as perfect as that of sample 4. It is apparent that the controlled high temperature crystallization process used for sample 4 has allowed the separate nucleation and growth of perfect cuboids, or equiaxed monoclinic crystals, whereas the other processes have on one hand produced a certain amount of lath-like crystals (sample 2), and in many cases produced bi-crystals and polycrystals (sample 3) as shown in Fig. 6. These latter crystals could have been formed by a change in crystal growth direction of one crystal, or more likely during the evaporation process, by either the nucleation of separate crystals on the surface of one which is already growing or the impingement of individual crystals during growth. Samples 2 and 3 can also be seen to contain many cracks within the crystals, and this again contrasts quite markedly with the well-defined product of the controlled crystallization process. However, it is anticipated that samples 2, 3 and 4 would behave in similar manners during subsequent processing.

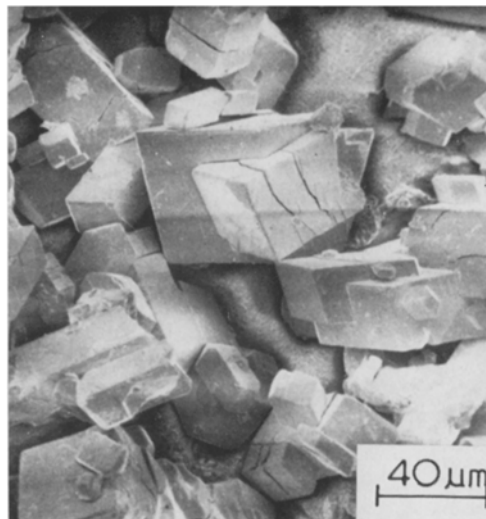


Figure 6 Sample 3 showing the existence of bicrystals and polycrystals.

4. Conclusions

(1) The three samples of APT, produced by crystallization from neutralized solutions of ammonia and tungstic acid at temperatures of the order of 70°C and above, have a monoclinic crystal structure, a cuboid or equiaxed-monoclinic particle morphology, and the chemical composition $5(\text{NH}_4)_2\text{O} \cdot 12\text{WO}_3 \cdot 5\text{H}_2\text{O}$.

(2) The sample of APT produced at room temperature by the neutralization of an ammonia and tungstic acid solution with hydrochloric acid has a lath-like particle morphology, an orthorhombic crystal structure, and has the chemical composition $5(\text{NH}_4)_2\text{O} \cdot 12\text{WO}_3 \cdot 11\text{H}_2\text{O}$.

(3) Solid APT produced by the freeze-drying of a tungstic acid and ammonia solution appears to be amorphous and to consist of very porous multiparticulate agglomerates. Thermogravimetric analysis indicates that this form of APT has the chemical composition $5(\text{NH}_4)_2\text{O} \cdot 12\text{WO}_3 \cdot 11\text{H}_2\text{O}$.

Acknowledgements

The authors would like to thank Professor E. Smith for the provision of laboratory facilities; the University of Manchester for a postgraduate award which enabled one of the authors (AKB) to carry out this work; High Speed Steel Alloys Ltd, Widnes for the supply of samples 1, 2 and 3; Wickman-Wimet Ltd, Coventry, for the supply of sample 4; and Crysus (Lancashire) Ltd, Chorley, for the supply of sample 5.

References

1. W. RYAN, "Non-ferrous extractive metallurgy in the United Kingdom" (Institution of Mining and Metallurgy, London, 1968) p. 194.
2. L. RAMQVIST, in "Modern Developments in powder metallurgy", edited by H. H. Hausner, Vol. 4 (Plenum Press, New York and London, 1971) p. 75.
3. A. LANDSBERG and T. T. CAMPBELL, *J. Metals*, **17** (1965) 856.
4. S. H. GELLES and F. K. ROEHRIG, *ibid*, **24** (1972) 23.
5. F. K. ROEHRIG and T. R. WRIGHT, *Mat. Eng.* **74** (1971) 17.
6. F. R. SALE, in "Fine Particles", edited by W. E. Kuhn and J. Ehretzman (The Electrochemical Society, New Jersey, 1974) p. 283.
7. M. C. KOSTELNIK and J. K. BEDDOW, in "Modern developments in powder metallurgy", edited by H. H. Hausner, Vol. 4 (Plenum Press, New York and London, 1971) p. 29.
8. R. HASEGAWA, T. KUROSAWA and T. YAGIHASHI, *Trans. Jap. Inst. Met.* **15** (1974) 75.
9. W. R. MORCOM, W. L. WORRELL, H. G. SELL and H. I. KAPLAN, *Met. Trans.* **5** (1974) 155.
10. J. C. NIEPCE and G. WATELLE-MARION, *Compt. Rend. Acad. Sci. Paris* **276** Series C (1973) 627.

Received 31 October and accepted 15 November 1974.